Proceedings of Engineering & Technology (PET)
pp. 851-866

Impact of DFIG based Wind Farms on Transient Stability of Power Systems

Mohamed Edrah, Kwok Lo, Abdussalam Elansari
co
University of Strathclyde
Glasgow, UK
mohamed.edrah@strath.ac.uk
abdussalam.elansari@strath.ac.uk

Omar .G. Mrehel
Department of Electronic & Electrical Engineering
University of Tripoli
Tripoli, Libya
O_rhoma@hotmail.com
O.Mrehel@uot.edu.ly

***Abstract*—As the installed capacity of wind power into power systems continues to grow, the effects of large-scale wind farms on stability of power systems becomes a serious concern. Conventional synchronous generators are increasingly replaced by wind turbines which have a different dynamic behaviour. Therefore, in this paper, the impacts of double fed induction generator (DFIG) based wind farms on transient stability of power systems are investigated. The transient behavior of a detailed model of large-scale DFIG wind farm is compared directly to the transient behavior of a conventional synchronous generator with the same rating. Moreover, a voltage control strategy of the DFIG rotor side converter (RSC) to support grid voltage is investigated. The study is carried out using the New England 10-machine 39-bus system with and without wind farm during a large grid disturbance. The simulation results show that DFIG based wind farms affect the transient stability of power systems. When a synchronous generator is replaced by a DFIG based wind farm the system transient stability is degraded to some extent.**

***Index Terms*—Doubly fed induction generator, power systems, synchronous generator, transient stability, wind turbine.**

I. Introduction

TRADITIONALLY Electricity was produced by using only synchronous generators. However, wind energy is now becoming the main renewable energy source of power. In recent years, the majority of wind farms that connected to the grid are equipped with DFIG. This kind of wind turbines is the most popular technology among several wind turbines technologies [1]. As the integration of DFIG into power system continuous to increase, there impact on power system transient stability becomes a main issue.

The DFIG consists of a wound rotor induction generator and back to back converter connecting the rotor slip rings to the grid. The active and reactive power output of the DFIG can be fully controlled by rotor side converter. The rating of rotor side converter and grid side converter of DFIG are about (25-30%) of the total wind power [2]. As the power converts controls the turbine output and decuples the machine from the grid, the behaviour of these machines during transient stability is different from that of synchronous generators. Therefore, the behaviour of the power systems could be significantly affected with the continuous increased of DFIG penetration.

Recently, an increased research effort is devoted to address the stability of power systems with wind power integration. According to [3] the transient stability of power system will be enhanced if a synchronous generator is replaced by DFIG wind turbine of the same capacity. However, the authors of [4] indicate that the power system transient stability is effected when a DFIG connected to the grid. Moreover, reference [5] advocates that replacing a conventional synchronous generator with a DFIG of the same rating can has a negative or positive impact on the power system transient stability.

During fault, voltage sags at DFIG terminal leads to a high current in rotor side converters. Since the converter rating is only about (25-30%) of the generator rating, the high current can damage the converter. For this reason, the converter systems have to be disconnected, the rotor windings are short circuited by crowbar protection system and hence the generator could be tripped. In this case, the DFIG will act as FSIG and hence the real and reactive power cannot be controlled [6].

The influence of wind generator reactive power on transient stability is examined by [7]. The study concluded that controlling wind generator reactive power to achieve a fixed terminal voltage value leads to better transient stability. Moreover, the reactive power generated from wind turbines has a positive impact on power system oscillations.

In this Paper, the impact of replacing conventional synchronous generator with a DFIG based wind farm on power system transient stability is analysed. The effect of wind farm active and reactive power, during transient stability period, on synchronous generators rotor angle is explored. The active and reactive power output of both synchronous generator and wind farm is compared. Moreover, the transient stability is investigated when the DFIG reactive power is controlled to achieve a certain voltage.

This paper is structured as follows: Section II describes the modelling of DFIG. Transient stability analysis is reviewed in section III. Section IV describes the test system. The results and discussion of a number of cases are outlined in section V. Finally, the paper conclusions are summarised in section VI.

ISSN: 2356-5608

II. MODELLING OF DFIG

The basic structure of a DFIG based wind turbine is shown in Fig. 1. The DFIG consists of a wound rotor induction generator and back to back converter connecting rotor slip rings to the grid. The wind turbine is connected to the induction generator through a mechanical shaft system. A gearbox is linking high and low speed shafts in the shaft system. The induction generator stator is directly connected to the grid whereas the rotor is fed through a back to back voltage source converter. The crow bar is used, during grid faults, to protect the rotor side converter from over current in the rotor circuit.

A. Aerodynamic Model

The extracted energy from the wind can be modelled by the aerodynamic model which is based on the coefficient of power. The maximum mechanical power that can be extracted from the wind kinetic energy is limited (Betz's limit) to 59.3% [8].

$$P_{ae} = 0.5\,\rho\,A\,v^{3}C_{p}\,(\lambda,\theta) \tag{1}$$

Where $\mathrm{Cp} = \dfrac{Extracted\ power}{Power\ in wind}$

In which P_{ae} is the aerodynamic power, ρ is the air density, A cross section of the air mass flow, v is the wind speed, C_p is the coefficient of power which depends on pitch angle θ and tip speed ratio λ [9].

$$\lambda = \frac{\omega_t R}{v} \tag{2}$$

Where, ω_t is the mechanical speed of the turbine, R is the rotor radius and v is wind speed.

B. Drive Train Model

The drive train contains the turbine rotor, gearbox, low and high speed shafts, and the induction generator rotor. The drive train can be modelled as two masses connected together by equivalent shaft stiffness. The two masses are the large turbine rotor (hub and blades) and the small generator (induction generator. The low speed aerodynamic torque, which is converted by stiffness model, is geared up to a torque on high speed shaft. A detailed description of drive train model can be found in [10, 11].

C. Generator Model

The generator that used in this study is a single cage wound rotor induction machine. The double-fed induction generator mathematical equations are the same as those of the fixed speed induction generator. The main difference is that the rotor voltage is not zero because the rotor windings are not shorted.

The induction generator stator and rotor equations can be written as follows:

$$\upsilon_{sabc} = R_s i_{sabc} + \frac{d\psi_{sabc}}{dt} \tag{3}$$

$$\upsilon_{rabc} = R_r i_{rabc} + \frac{d\psi_{rabc}}{dt} \tag{4}$$

Applying synchronous reference frame transformation rotating by angular speed to above equations, The differential equations of the DFIG induction machine in d-q are [12, 13]:

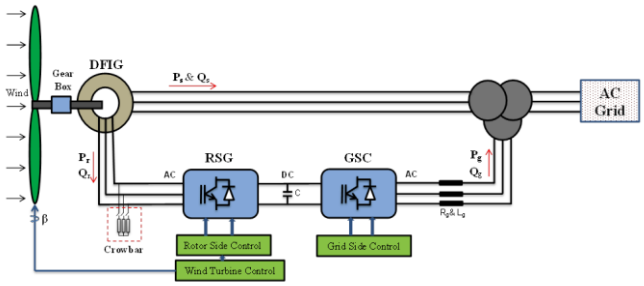

Fig. 1. General structure of DFIG wind turbine with controls

Stator and rotor voltage equations in d-q axis:

$$\upsilon_{ds} = R_s i_{ds} + \omega_s \psi_{ds} + \frac{d\psi_{ds}}{dt} \tag{5}$$

$$\upsilon_{qs} = R_s i_{qs} + \omega_s \psi_{qs} + \frac{d\psi_{qs}}{dt} \tag{6}$$

$$\upsilon_{dr} = R_r i_{dr} - (\omega_s - \omega_r)\psi_{dr} + \frac{d\psi_{dr}}{dt} \tag{7}$$

$$\upsilon_{qr} = R_r i_{qr} + (\omega_s - \omega_r)\psi_{qr} + \frac{d\psi_{qr}}{dt} \tag{8}$$

Where $\upsilon_{qs}, i_{qs}, \psi_{qs}$ are stator voltage, current and flux linkage in the q axis, and $\upsilon_{qr}, i_{qr}, \psi_{qr}$ are the rotor voltage, current and flux linkage in the q axis. $\upsilon_{ds}, {}_s\, i_{ds}, \psi_{ds}$ are the stator voltage, current and flux linkage in the d axis, and $\upsilon_{dr}, i_{dr}, \psi_{dr}$ are the rotor voltage, current and flux linkage in the d axis. ω_s and ω_r are rotational speed of the synchronous reference frame and the rotor speed.

Flux linkage equations in d-q axis:

$$\psi_{ds} = L_{ls} i_{ds} + L_m (i_{ds} + i_{dr}) = L_s i_{ds} + L_m i_{dr} \tag{9}$$

$$\psi_{qs} = L_{ls} i_{ds} + L_m (i_{qs} + i_{qr}) = L_s i_{qs} + L_m i_{qr} \tag{10}$$

$$\psi_{dr} = L_{lr} i_{dr} + L_m (i_{ds} + i_{dr}) = L_r i_{dr} + L_m i_{ds} \tag{11}$$

$$\psi_{qr} = L_{lr} i_{dr} + L_m (i_{qs} + i_{qr}) = L r i_{qr} + L_m i_{qs} \tag{12}$$

Where the stator L_s and rotor L_r inductance are defined by:

$$L_s = L_{ls} + L_m\,,\ L_r = L_{lr} + L_m \tag{13}$$

In the above flux linkage equations, L_m is the mutual inductance and L_{ls}, L_{lr} are the stator and rotor leakage inductance.

By neglecting the stator and rotor power losses, the equations of active and reactive power are:

$$P_s = \frac{3}{2}(\upsilon_{ds} i_{ds} + \upsilon_{qs} i_{qs}), \quad Q_s = \frac{3}{2}(\upsilon_{qs} i_{ds} - \upsilon_{ds} i_{qs}) \tag{14}$$

$$P_r = \frac{3}{2}(\upsilon_{dr} i_{dr} + \upsilon_{qr} i_{qr}), \quad Q_r = \frac{3}{2}(\upsilon_{qr} i_{dr} - \upsilon_{dr} i_{qr}) \tag{15}$$

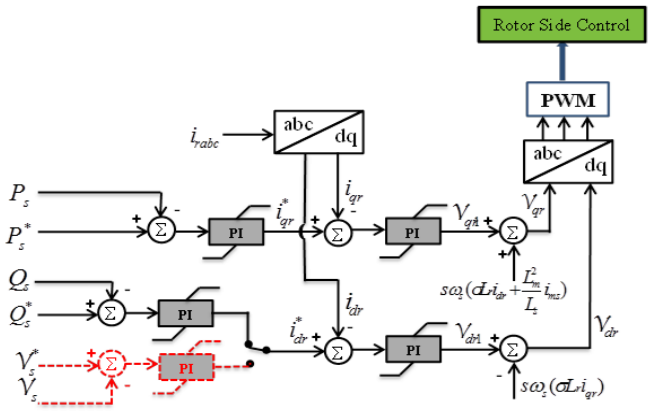

Fig. 2. Overall vector control scheme of the DFIG rotor side converter, voltage control strategy (dashed red lines).

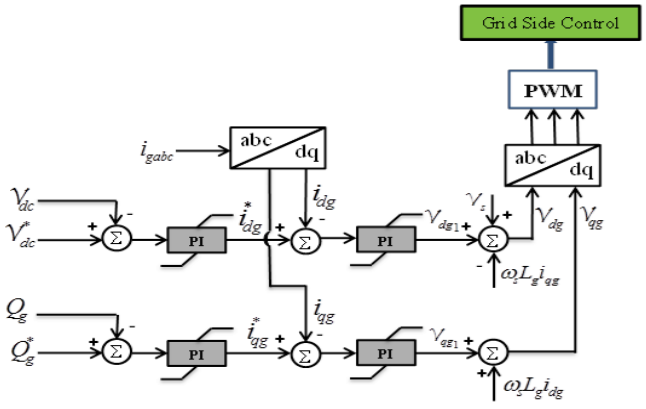

Fig. 3. Overall vector control scheme of the DFIG ststor side converter.

The torque in d-q is given by the following equation:

$$T_e = \psi_{ds} i_{qs} - \psi_{qs} i_{ds} = \psi_{qr} i_{dr} - \psi_{dr} i_{qr} = L_m (i_{qs} i_{dr} - i_{ds} i_{qr}) \quad (16)$$

Where T_e is the electromagnetic torque that developed by the induction generator.

D. Power Converters Model

The power converters of DFIG consist of RSC and GSC as shown in Fig. 1. The RSC rating depends on two factors, reactive power control limits and the maximum slip. Whereas, the GSC rating depends on maximum slip only because it usually operate at unity power factor [14].

The main objective of RSC is to regulate the stator side active and reactive power independently. DFIG stator voltage can be regulated to achieve a certain limit by controlling the reactive power through RSC. The voltage control outer loop is marked as black dashed lines in Fig. 2. The rotor side power converter can be modelled as a current controlled voltage source converter. There is a several ways to control and supply a sinusoidal current at rotor frequency. The common method is by using pulse width modulation (PMW) [14].

The control of DFIG stator active power P_s and reactive power Q_s is achieved by controlling the rotor current i_{rabc} in the stator flux oriented reference frame. The control of DFIG stator active power P_s and reactive power Q_s is achieved by controlling the rotor current i_{rabc} in the stator flux oriented reference frame [15].

The main objective of GSC is to control the voltage of DC link to maintain it within the certain limit. However, it can regulate the reactive power that GSC exchange with the grid to be used to support the grid during a fault [16].

The overall vector control scheme of the GSC is shown in Fig. 3, in which the stator current i_{gabc} in the synchronously rotating reference frame is used to control the DC voltage (v_{dc}) and the reactive power Q_g that can be exchanged between the grid and the GSC. The grid current i_{gabc} are transferred to d-q current component i_{dg} and i_{qg} by applying the synchronously rotating reference frame. In a similar way to the RSC, the GSC has two control loops which are outer control and inner control loops[17], [15].

E. Pitch Angle Controller

The pitch angle controller is used to reduce the mechanical power that extracted from the wind and to prevent the turbine from over speeding. Therefore, turbine blade pitch control is only activated at high wind. Fig. 4 shows the wind turbine blade pitch control, where $P_e = (P_s + P_g)$ and ω_r are the output active power and the rotating speed of DFIG respectively [18].

If the wind turbine is required to generate its maximum power during low speed wind the ω_r and P_e are set at their reference values. Therefore, the blade pitch control is deactivated in this situation. However, if the wind turbine is required to generate a constant amount of power less than its maximum power rating, the active power controller may be activated [12].

The bitch angle is adjusted by the active power controller to lessen the extracted mechanical power. As a result, the difference between the mechanical and electrical power is reduced. However, when the wind speed exceeds the turbine rated value, both of the speed and active power controls are activated.

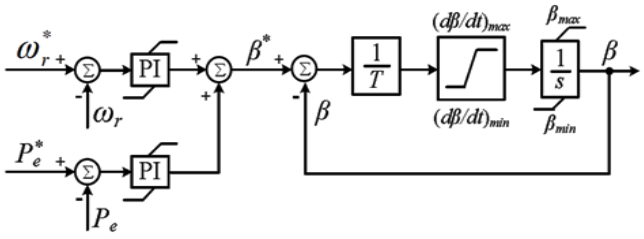

Fig. 4. DFIG wind turbine blade pitch control.

III. TRANSIENT STABILITY ANALYSIS

Transient stability is the ability of the power system to remain synchronised after being subjected to a severe disturbance. To conduct a transient stability analysis, the examined system has to be exposed to a large disturbance such as three-phase short circuit fault. The time domain for transient angle stability studies is between 3 s to 5 s and can be extended

to 10 s for large power systems. It can be measured by transient stability index (TSI) [19].

$$\eta = \frac{360^{o} - \delta_{\max}}{360^{o} + \delta_{\max}} \times 100 \qquad Where \qquad -100 < \eta < 100$$

(17)

Where: η and $\delta_{\max}$ are transient stability index symbol and maximum angle separation (in degree) between any two synchronous generators in the system at the same time respectively. The power system considered as a stable system if the value of η is greater than zero.

IV. TEST SYSTEM

The New England 10-machine 39-bus system was used to study the impact of a DFIG wind farm on power system transient stability as shown in Fig. 5 [20]. The system consists of 10 synchronous generators, 12 transformer, 46 transmission lines and 19 loads. All synchronous machines are equipped with (TGOV1) turbine governor, (IEEEX1) exciter and (STAB1) power system stabilizer. The static and dynamic data of the test system can be found in [21] .

To investigate the influence of DFIG wind turbines on the power system transient stability, a large-scale DFIG wind farm is connected to the test system. A time domain simulation with a detailed model of synchronous generators and DFIG based wind farm is used to assess the transient stability of the system with and without wind farm. For this purpose, the test system and the DFIG wind turbine are modelled and simulated by using NEPLAN software [22]. The three loads were modelled as 33% constant current, 33% constant power and 33% constant impedance [23].

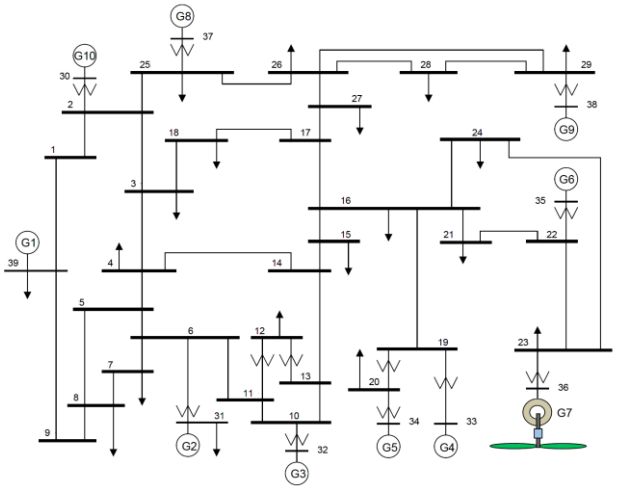

Fig. 5. Single line diagram of the test system with DFIG based wind farm.

In this paper, the synchronous generator G_7 is replaced by a similar rating large-scale wind farm. The wind farm consists of 5 MW 112 wind turbine aggregated into a two large DFIG wind turbines. The DFIG based wind farm generates 560 MW which is similar amount to that generated from synchronous machine G7. The aggregation method used to aggregate the wind turbines in this study is explained in [24].

V. RESULTS AND DISCUSSION

In this paper, three different cases are analysed by a time domain simulator to show the impact of DFIG on power systems transient stability. The description of each case is as following:

- **Case A:** in this case, there is no wind power connected to the test system. It is a base case in which the all generators are conventional synchronous generators.
- **Case B:** in this case, the synchronous generator G7 is replaced by a large-scale DFIG based wind farm with an equivalent rating. The wind farm is operating at a unity power factor (no reactive power is exchanged between the test system and the wind farm).
- **Case C:** in this case, the synchronous generator G7 is replaced by a large-scale DFIG based wind farm with an equivalent rating. The wind farm is operating on voltage control mode controlling its terminal voltage at a certain value. The terminal voltage controlled at 1.0635 pu, which is the same value as the replaced synchronous generator G_7.

To conduct a transient stability analysis, the test system exposed to a three-phase short circuit fault. The location of the disturbance is selected to be near the critical bus 16. A three-phase fault of 150 ms is created near bus 16 at the transmission line connecting bus 16 and bus 24. The fault is cleared out by disconnecting the faulty line from both sides.

To study the influence of DFIG based wind farm on the transit stability of the test system, rotor angle of each generator is observed. Then the transient stability index of the test system can be calculated from these rotor angles. The angle of the synchronous generator G_2, which is a slack machine, was

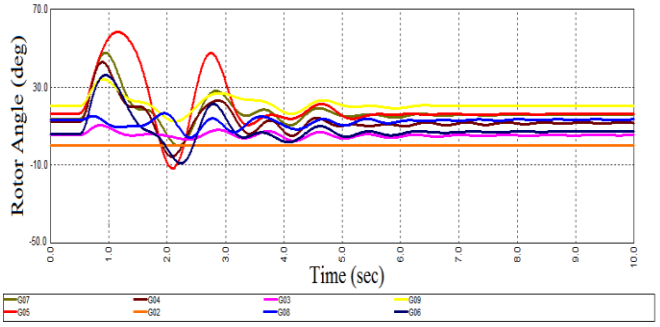

Fig. 6. Rotor angle of each synchronous generator of the test system.

chosen as a reference angle. Active and reactive power outputs of critical angle generators are monitored. Moreover, Active and reactive power of wind farm are absorbed to be compared to the replaced synchronous generator. Furthermore, the terminal voltage of buses 16 and 23 are monitored.

Fig. 6 shows the individual rotor angle variation of each synchronous machine. It can be seen that the system is stable and the rotor angle oscillation is damped by the equipped power system stabilizers. However, rotor angle of machines

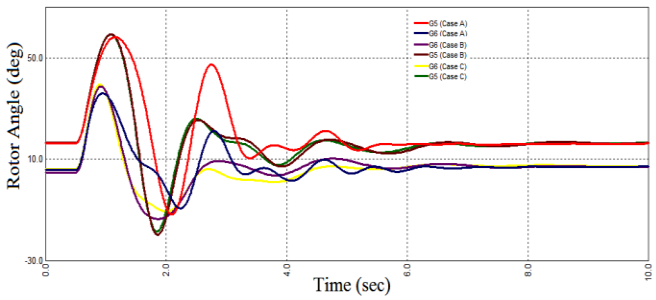

Fig. 7. Rotor angle of G_5 and G_6 for each case.

TABLE I
TRANSIENT STABILITY INDEX OF CASES A-C

TSI	Case A	Case B	Case C
η	72.15	71.71	71.86

(G_4, G_5, G_6, G_7), which are near the faulted location are critical. Therefore, the rotor angles of machines (G_5, G_6) are used to observe the transient stability of the three cases.

In Fig. 7, the rotor angle of (G_5, G_6) relevant to G_2 is compared for the three cases. It is clear that the rotor angle deviation of the two synchronous generators in cases (B, C) is different from the first case. This different is due to the fact that wind farm cannot influence the system electromagnetic torque. There is a little to no improvement when the wind farm controlling the voltage of point of common coupling. However, the oscillation of the rotor angle in case C is damping better than the case B. Table I shows the transient stability index for the three cases. From the table, it is clear that the transient stability of the power system is reduced if a synchronous generator is replaced by an equivalent rated wind farm equipped with a DFIG.

Terminals voltage of faulted bus (N16) and the terminal bus (N23) of wind farm and replaced synchronous generator are shown in Fig 8. The voltage of faulted bus is falls to about 6 pu then recovers quickly, after the fault, to the normal value. The voltage behaviour at the faulted bus is similar in the three cases before, during after the fault is cleared out. However, the terminal voltage (N23) of wind farm and G_7 is different during and after the fault as can be seen in Fig 8b. During the fault, the voltage of G_7 drops to 0.36 pu then improves quickly after the fault. However in the case of wind farm the voltage falls to 0.2 pu during the fault then reaches about 0.8 pu after the fault and during the time when the crowbar protection is still on. After the crowbar protection deactivated the voltage recovers to the normal value in case C when the wind farm terminal voltage is controlled. This different in the voltage behaviour of bus (N23) between the three cases is due to the reactive power variation in each case as can be seen in Fig 9. Because of synchronous generator reactive power capability, G_7 is able to provide a reactive power during the fault period. However, in the cases of wind farm, no reactive power is injected to the grid. Conversely, the wind farm absorbs a large amount of reactive power especially during the active time of crowbar protection.

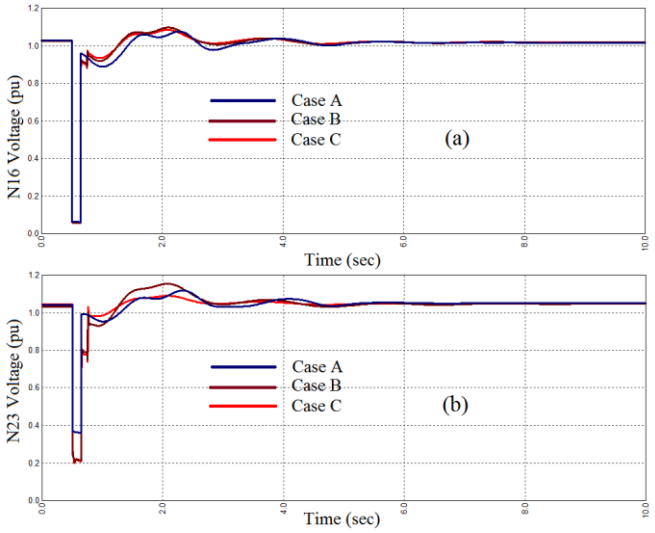

Fig. 8. Voltage of (a) faulted bus (N16) and Generator's terminal voltage (N23) for each case.

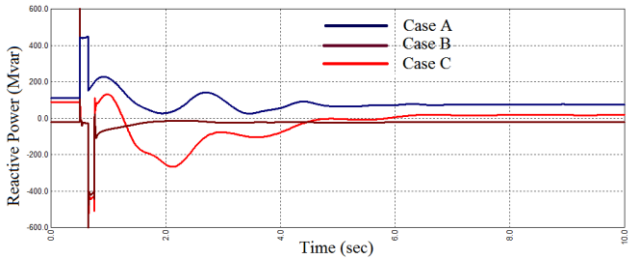

Fig. 9. Total reactive power of G_7 and wind farm for each case.

When the terminal voltage of the wind farm is controlled the reactive power output is variable to keep the voltage at a predefined value after the fault and when the crowbar deactivated. However, in case B, the wind farm reactive power output almost zero.

Active power of each case can be seen in Fig. 10. The active power output of G_7 is different during and after the fault is cleared from the wind farm cases. G_7 is providing the grid with about 100 MW of active power during the fault period compared to just 26 MW injected from the wind farm. Conversely, the active power of synchronous generator G_7, after the fault, is changeable due to its inertia response.

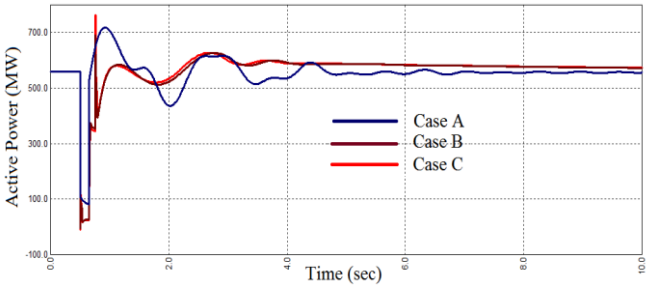

Fig. 10. Total active power of G_7 and wind farm for each case.

However, in the case of wind farm, the active power output after the fault is relatively smooth.

VI. CONCLUSIONS

In this paper, the impacts of DFIG based wind farms on transient stability of power systems are examined. A detailed model of both DFIG and synchronous generator is used to analysis the transient stability of the test system under a large disturbance. From the results of time domain simulator, it is clear that the DFIG based wind farms affect the transient stability of power systems. When the synchronous generator is replaced by a DFIG based wind farm operating at a unity power factor, the system transient stability is degraded to some extent. However, replacing a synchronous generator by a DFIG based wind farm that used the reactive power to control its terminal voltage has less negative impact.

Results are also showed that synchronous generator can produce reactive power during the complete period of fault to support the grid voltage. However, in the case of wind farm a large amount of reactive power is absorbed leading to a further voltage drop. However, the wind farm active power is more stable after the fault than that of synchronous generator. This is due to the reason that DFIG provides negligible inertial response.

REFERENCES

[1] R. Datta and V. T. Ranganathan, "Variable-speed wind power generation using doubly fed wound rotor induction machine-a comparison with alternative schemes," Energy Conversion, IEEE Transactions on, vol. 17, pp. 414-421, 2002.

[2] M. V. Nunes, J. Peas Lopes, H. H. Zurn, U. H. Bezerra, and R. G. Almeida, "Influence of the variable-speed wind generators in transient stability margin of the conventional generators integrated in electrical grids," Energy Conversion, IEEE Transactions on, vol. 19, pp. 692-701, 2004.

[3] C. Huizhu and L. Yanhua, "Impact of large scale wind farm integration on power system transient stability," Automation of Electric Power Systems, vol. 15, p. 004, 2006.

[4] L. Shi, S. Dai, Y. Ni, L. Yao, and M. Bazargan, "Transient stability of power systems with high penetration of DFIG based wind farms," in Power & Energy Society General Meeting, 2009. PES'09. IEEE, 2009, pp. 1-6.

[5] C. Samarasinghe and G. Ancell, "Effects of large scale wind generation on transient stability of the New Zealand power system," in Power and Energy Society General Meeting-Conversion and Delivery of Electrical Energy in the 21st Century, 2008 IEEE, 2008, pp. 1-8.

[6] Q. Wei and R. G. Harley, "Effect of grid-connected DFIG wind turbines on power system transient stability," in Power and Energy Society General Meeting - Conversion and Delivery of Electrical Energy in the 21st Century, 2008 IEEE, 2008, pp. 1-7.

[7] E. Vittal, M. O'Malley, and A. Keane, "Rotor Angle Stability With High Penetrations of Wind Generation," Power Systems, IEEE Transactions on, vol. 27, pp. 353-362, 2012.

[8] T. Ackermann, Wind Power in Power Systems: John Wiley & Sons, Ltd, 2005.

[9] O. Anaya-Lara, N. Jenkins, J. Ekanayake, P. Cartwright, and M. Hughes, Wind Energy Generation: Modelling and Control: Wiley, 2009.

[10] A. D. Hansen, P. Sørensen, F. Blaabjerg, and J. Becho, "Dynamic modelling of wind farm grid interaction," Wind Engineering, vol. 26, pp. 191-210, 2002.

[11] C. Jauch, P. Sørensen, I. Norheim, and C. Rasmussen, "Simulation of the impact of wind power on the transient fault behavior of the Nordic power system," Electric Power Systems Research, vol. 77, pp. 135-144, 2007.

[12] Q. Wei, "Dynamic modeling and control of doubly fed induction generators driven by wind turbines," in Power Systems Conference and Exposition, 2009. PSCE '09. IEEE/PES, 2009, pp. 1-8.

[13] J. Zhenhua and Y. Xunwei, "Modeling and control of an integrated wind power generation and energy storage system," in Power & Energy Society General Meeting, 2009. PES '09. IEEE, 2009, pp. 1-8.

[14] R. Pena, J. C. Clare, and G. M. Asher, "Doubly fed induction generator using back-to-back PWM converters and its application to variable-speed wind-energy generation," Electric Power Applications, IEE Proceedings -, vol. 143, pp. 231-241, 1996.

[15] L. Qu and W. Qiao, "Constant power control of DFIG wind turbines with supercapacitor energy storage," Industry Applications, IEEE Transactions on, vol. 47, pp. 359-367, 2011.

[16] E. Tremblay, A. Chandra, and P. Lagace, "Grid-side converter control of DFIG wind turbines to enhance power quality of distribution network," in Power Engineering Society General Meeting, 2006. IEEE, 2006, p. 6 pp.

[17] Q. Wei, G. K. Venayagamoorthy, and R. G. Harley, "Real-Time Implementation of a STATCOM on a Wind Farm Equipped With Doubly Fed Induction Generators," Industry Applications, IEEE Transactions on, vol. 45, pp. 98-107, 2009.

[18] Q. Wei, Z. Wei, J. M. Aller, and R. G. Harley, "Wind Speed Estimation Based Sensorless Output Maximization Control for a Wind Turbine Driving a DFIG," Power Electronics, IEEE Transactions on, vol. 23, pp. 1156-1169, 2008.

[19] S. Libao, D. Shiqiang, N. Yixin, Y. Liangzhong, and M. Bazargan, "Transient stability of power systems with high penetration of DFIG based wind farms," in Power & Energy Society General Meeting, 2009. PES '09. IEEE, 2009, pp. 1-6.

[20] T. Athay, R. Podmore, and S. Virmani, "A Practical Method for the Direct Analysis of Transient Stability," Power Apparatus and Systems, IEEE Transactions on, vol. PAS-98, pp. 573-584, 1979.

[21] M. A. Pai, Computer techniques in power system analysis: Tata McGraw-Hill Publishing Company, 1979.

[22] B. B. C. P. Inc. "NEPLAN® Power System Analysis and Engineering", . Available: http://www.neplan.ch/html/e/e_home.htm

[23] "Standard load models for power flow and dynamic performance simulation," Power Systems, IEEE Transactions on, vol. 10, pp. 1302-1313, 1995.

[24] L. M. Fernandez, C. A. Garcia, J. R. Saenz, and F. Jurado, "Reduced model of DFIGs wind farms using aggregation of wind turbines and equivalent wind," in Electrotechnical Conference, 2006. MELECON 2006. IEEE Mediterranean, 2006, pp. 881-884.